

The University of Bradford Institutional Repository

<http://bradscholars.brad.ac.uk>

This work is made available online in accordance with publisher policies. Please refer to the repository record for this item and our Policy Document available from the repository home page for further information.

To see the final version of this work please visit the publisher's website. Access to the published online version may require a subscription.

Link to publisher's version: <https://doi.org/10.1007/s11069-018-3168-4>

Citation: Hanmaiahgari PR, Gompal NR, Pal D et al (2018) Numerical modelling of the Sakuma Dam reservoir sedimentation. *Natural Hazards*. 91(3): 1075-1096.

Copyright statement: © Springer Science+Business Media B.V., part of Springer Nature 2018. Reproduced in accordance with the publisher's self-archiving policy. This is a post-peer-review, pre-copyedit version of an article published in *Natural Hazards*. The final authenticated version is available online at: <https://doi.org/10.1007/s11069-018-3168-4>.

Numerical modeling of the Sakuma Dam reservoir sedimentation

Prashanth R. Hanmaiahgari*, Nooka Raju Gompal, Debasish Pal, Jaan H Pu

*Prashanth Reddy Hanmaiahgari, Assistant Professor, Dept. of Civil Eng., Indian Institute of Technology Kharagpur, Kharagpur, West Bengal, India 721302. E-mail: hpr@civil.iitkgp.ernet.in (corresponding author)

Nooka Raju Gompal, Graduate student, Dept. of Civil Eng., Indian Institute of Technology Kharagpur, Kharagpur, West Bengal, India 721302. E-mail: rajugompal@gmail.com

Debasish Pal, Department of Civil Engineering, Indian Institute of Technology Kharagpur, Kharagpur 721302, India, Present Address: Engineering Systems and Design Pillar, Singapore University of Technology and Design, 8 Somapah Road, Singapore 487372, Singapore. E-mail: bestdebasish@gmail.com

J H Pu, Lecturer, School of Engineering, Faculty of Engineering and Informatics, University of Bradford, Bradford BD7 1DP, United Kingdom. E-mail: J.H.Pu1@bradford.ac.uk

Abstract

The present study attempts to predict the reservoir sedimentation in 32 km region of the Tenryu River between the Hiraoka and Sakuma Dams in Japan. For numerical simulations of the reservoir sedimentation, the one-dimensional model of the Hydrologic Engineering Centre-River Analysis System (HEC-RAS) is used together with the inclusion of channel geometry, bed gradation curve, Exner-5 bed sorting mechanisms, fall velocity of the particle, and flow and sediment boundary conditions pertaining to modeling region. The modeling region of the Tenryu River is divided into 48 river stations with 47 reaches in the numerical simulations. The numerical model is calibrated using the available data for 48 years from 1957 to 2004. The formulae of sediment transport function, Manning's roughness coefficient, computational increment and fall velocity have been identified for getting the best estimation of the Sakuma Dam reservoir sedimentation. Combination of obtained sensitive parameters and erodible limits of 2 m gave the best comparison with the measured bed profile. The computed results follow the trend of measured data with a small under estimation. Although, Manning's roughness coefficient has an effect on the sedimentation, no direct relation is found between the Manning's roughness coefficient and reservoir sedimentation. It is found that the temperature of water has no effect on the reservoir sedimentation.

Keywords: Reservoir sedimentation, Numerical modeling, HEC-RAS, Tenryu River, Hiraoka Dam, Sakuma Dam.

1. Introduction

Reservoir sedimentation is an important research topic as it has direct application in dam construction, flow regulation, flood control, navigation, hydropower, water supply and many other issues related to environmental benefits. In recent years, a voluminous amount of research in predicting the reservoir sedimentation has been performed from empirical, semi-empirical and numerical viewpoints (Ching-Hsein et al., 2012; Caputo and Carcione, 2013; Haun et al., 2013; Tsai et al., 2014; Ahm and Yang, 2015; Hosseinzadeh et al., 2015; Issa et al., 2016; Ji et al., 2016; Lauer et al., 2016). Chen et al. (2015) developed and demonstrated a mathematical model for sediment deposition and erosion in a river during flood events. Yin et al. (2016) used the established hydrodynamic and sediment model (Delft3D) to accurately predict the siltation in the Hengmen Eastern Access Channel (HEAC) in China during a storm surge. In our society, due to the immense importance of a river flow and impacts of designing a dam on its path, a more case-specific investigations of fluvial sediment transport, reservoir sedimentation and bathymetric changes are highly required. Sediment transport can be investigated using one-dimensional, two-dimensional and three-dimensional numerical models; however Molinas and Yang (1986) pointed out that the two-dimensional and three-dimensional models require a large data for calibration and an excessive computational time whereas one dimensional model can solve the problem with a lesser computational resource. In the system of river flow, the length scale is very large in comparison to the width scale, therefore it can be assumed that the flow is dominantly in one direction and a one-dimensional model can deliver accurate results in the simulations of sediment transport; however the sediment sorting in meandering river cannot be modeled with a one-dimensional model.

The sediment reaching the reservoir per unit time is expressed as a summation of bed load and suspended load. The sediment dynamics depend on the shape, size and type of sediment particles, drainage area, climate change, flood magnitude, slope of the river basin, vegetation in the catchment area, braided river system and several other factors (Morris and Fan 1998). Apart from this, the discharge of sediment is also affected by turbulence characteristics of flow, grain-size distribution of bed material, armoring of bed, hydrological cycle, temperature of water, cross-sectional shape of channel, bed roughness and other features (Yang, 2006). Palmieri et al. (2003) considered 4000 dams together with their approximate reservoir volume of 7000 km³ and showed that almost 45 km³ (0.5% - 1%) volume of water storage was lost annually due to the

sedimentation. Haq and Abbas (2007) found that the Tarbela reservoir of Pakistan, which was built in 1974 with the initial storage capacity of 14.34 km^3 , is receiving a sediment volume of 0.132 km^3 annually and without proper sediment inflow countermeasures, the dam would lose its useful life in less than a century (Beebo and Bilal 2012). The decrease in reservoir storage due to sediment deposits has a significant impact on the water supply to irrigation and drinking water, which can be ascertained by the example of the Camaré irrigation reservoir in Venezuela, where the storage volume was exhausted in just 15 years (Morris and Fan 1998; Beebo and Bilal 2012; Harb, 2013). Therefore, indeed it is important to implement the best real life sediment management practices in other existing important reservoirs and the Sakuma Dam is one of them which is located on the Tenryu River in Japan.

Chaishi et al. (2002) studied the accumulation of sediment and its countermeasures in the Sakuma Dam reservoir. Okano et al. (2005) discussed the sediment deposition in the reservoir of the Sakuma Dam and its effect on the bed changes of the Tenryu River. The sloping terrain and frail geological composition of the catchment area are responsible for the large sediment discharge into the Tenryu River and it was observed that the sediment concentration is small in the discharged water from the Sakuma Dam; therefore in the downstream of the dam, the river bed is eroded for energy balance and results in 1-1.5 m degradation of the bed (Sato and Liu, 2008). The eroded sand bypassing at the Sakuma Dam against the decay of the Tenryu River delta coast was investigated by Miyahara et al. (2010). Huang (2011) proposed a new relationship between suspended sediment and the carrying capacity of the channel together with the morphological characteristics of the Sakuma Dam. Using the Hydrologic Engineering Centre-River Analysis System (HEC-RAS), numerical simulations of bathymetric changes in the Tenryu River due to reservoir sedimentation of the Sakuma Dam were carried out by Beebo and Bilal (2012).

Apart from the aforementioned studies, it needs to be mentioned here that till date, a comprehensive study on the reservoir sedimentation of the Sakuma Dam has not been carried out by including various bed gradation curves, bed sorting mechanisms, channel geometry, roughness coefficients, sediment transport functions, temperature of water, and flow and sediment boundary conditions. This paper aims at carrying out a detailed numerical study of the Sakuma Dam reservoir sedimentation using the one-dimensional model HEC-RAS. The paper is organized as follows. The detailed methodology of numerical simulations has been presented in Section 2. A short description of the Sakuma Dam and its relevant features are given in Section

3. The calibration of the model with field measurements is explained in Section 4. The obtained results and the corresponding discussion is presented in Section 5. A summary of conclusions is provided at the end of the paper.

2. Methodology

2.1. HEC-RAS

The HEC-RAS model was developed by the Hydrologic Engineering Center, which is a part of the Institute for Water Resources, U. S. Army Corps of Engineers, Davis, California. The software was released in 1995 and initially it was a one-dimensional numerical model for the computation of water surface profiles in steady and unsteady flow in a non-prismatic channel together with gradually varied profile, rapidly varied profile and mixed profile. After that, HEC-RAS was enhanced for the analysis of water quality and the computation of sediment transport together with the movable boundary condition. The advantage of HEC-RAS is that it is developed based on an object oriented programming and the objects are shared by different subroutines without data duplication (Brunner, 2002 a, b). In this paper, HEC-RAS 5.0 Beta version which was launched in October 2014 was used for the numerical simulations.

2.2. Governing Equations

The one-dimensional Saint-Venant equations were the governing equations for this study. For unsteady flow in a prismatic open channel with erodible sediment bed, the continuity equation of flowing water can be written as

$$\frac{\partial A}{\partial t} + \frac{\partial Q}{\partial x} - q_l = 0 \quad (1)$$

and the momentum equation of water flow as follows

$$\frac{\partial Q}{\partial t} + \frac{\partial(VQ)}{\partial x} + gA \left(\frac{\partial z}{\partial x} + S_f \right) = 0 \quad (2)$$

where x is the flow direction, t is the time, A is the cross-section, V is the average flow velocity, Q is the discharge in the channel, q_l is the lateral discharge per unit length along the channel, $-\frac{\partial z}{\partial x}$ is the channel bottom slope and S_f is the slope of frictional loss. Apart from Eqs. (1) and (2), the Exner equation states the conservation of mass and it is applied to the sediment volume in fluvial flow. The Exner equation is written as

$$(1 - \lambda) \frac{\partial \eta}{\partial t} = - \frac{\partial Q_s}{\partial x} \quad (3)$$

where η is the bed elevation, λ is the bed porosity and Q_s is the sediment flux. Equation (3) is solved by computing the sediment transport capacity in the control volume and comparing it with the sediment inflow into the control volume. The greater and lesser values of sediment transport capacity in comparison to the incoming discharge result in erosion and deposition of the sediment bed respectively.

2.3. Numerical Scheme

HEC-RAS uses Preissmann Scheme, which is a four point implicit finite difference scheme developed for the discretization of the governing equations (Brunner, 2002 a, b). Moreover, the scheme can be used for spatial discretization of the variable. A schematic diagram of the finite difference grid is shown in Fig. 1. The implicit finite difference scheme with a weighted factor α is given by

$$f_j = f_j^k \quad (4)$$

$$\Delta f_j = f_j^{k+1} - f_j^k \quad (5)$$

$$\text{Time derivative, } \frac{\partial f}{\partial t} \approx \frac{\Delta f}{\Delta t} = \frac{1}{\Delta t} \left(\frac{\Delta f_{j+1} + \Delta f_j}{2} \right) \quad (6)$$

$$\text{spatial derivative, } \frac{\partial f}{\partial x} \approx \frac{\Delta f}{\Delta x} = \left(\frac{(f_{j+1} - f_j) + \alpha(\Delta f_{j+1} - \Delta f_j)}{\Delta x} \right) \quad (7)$$

$$\text{function value, } f = 0.5(f_{j+1} - f_j) + 0.5\alpha(\Delta f_{j+1} - \Delta f_j) \quad (8)$$

In Eqs. (4) to (8), f represents dependent variables V , h and η etc. and the steep wave fronts can be computed by varying the weighting factor α . The finite difference scheme is unstable for $\alpha < 0.5$, conditionally stable for $\alpha = 0.5$ and unconditionally stable for $0.5 < \alpha < 1$.

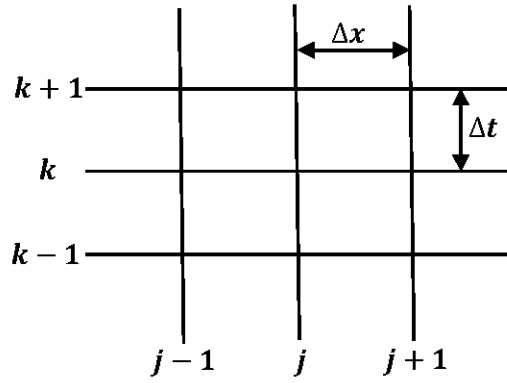


Figure 1: Schematic diagram of finite difference grid.

2.4. Input Data

This section describes the geometric Data, hydraulic boundary condition, sediment data and sediment boundary condition which are the inputs required for modeling with HEC-RAS.

2.4.1. Geometric Data

The geometric data required to create a model in HEC-RAS consists multiple cross-sections of a river and reaches in between them. The cross-sections are linked together to create the modeling region of the river. A scaled diagram of the modeling region was created in HEC-RAS; however, due to the one-dimensional nature, the diagram shows only the sequence of the cross-sections.

2.4.2. Hydraulic Boundary Conditions

In this study, the simulations of sediment transport were carried out by the quasi-unsteady hydraulic data. The types of flow boundary conditions available in HEC-RAS include Flow Series, Lateral Flow Series, Uniform Lateral Flow, Normal Depth, Stage Series, Rating Curve, and Time Series Gate Openings. Moreover, the water temperature needs to be provided to run a sediment transport model. Further, HEC-RAS uses a hydrodynamic simplification called quasi-unsteady approximation which converts the continuous hydrograph into a series of discrete steady flow profiles. For convenience, a schematic diagram of approximation is shown in Fig. 2.

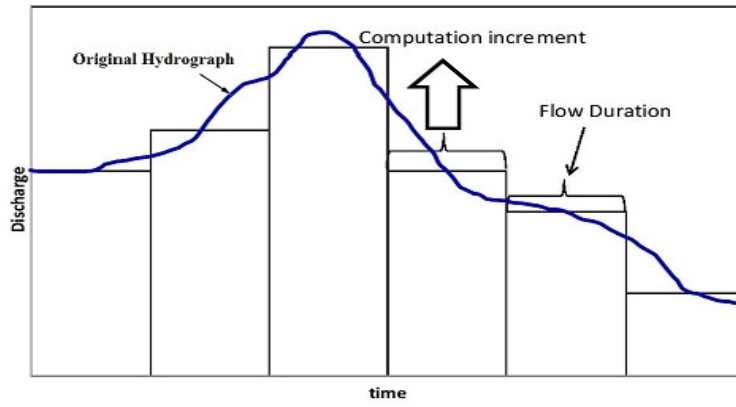
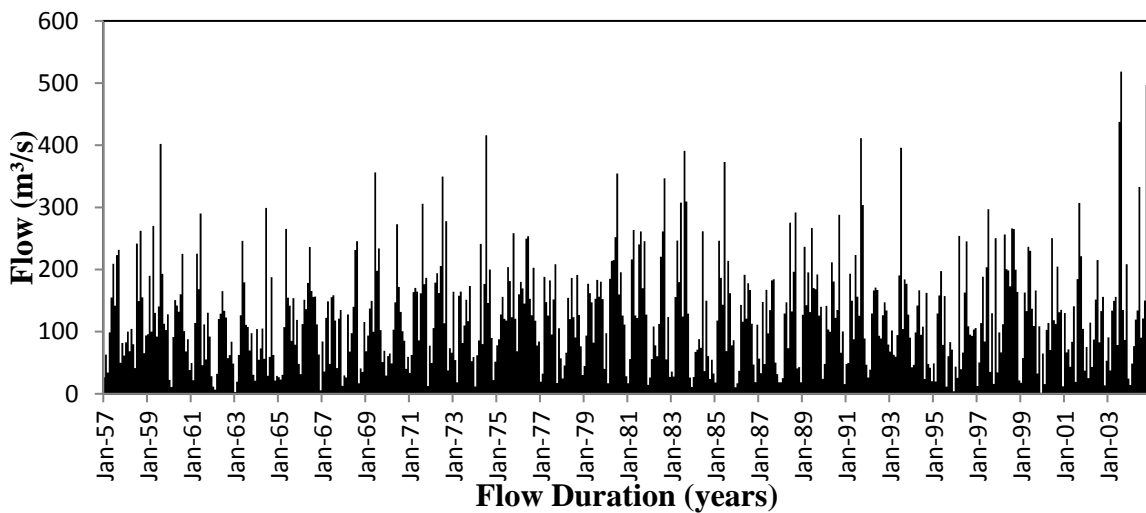
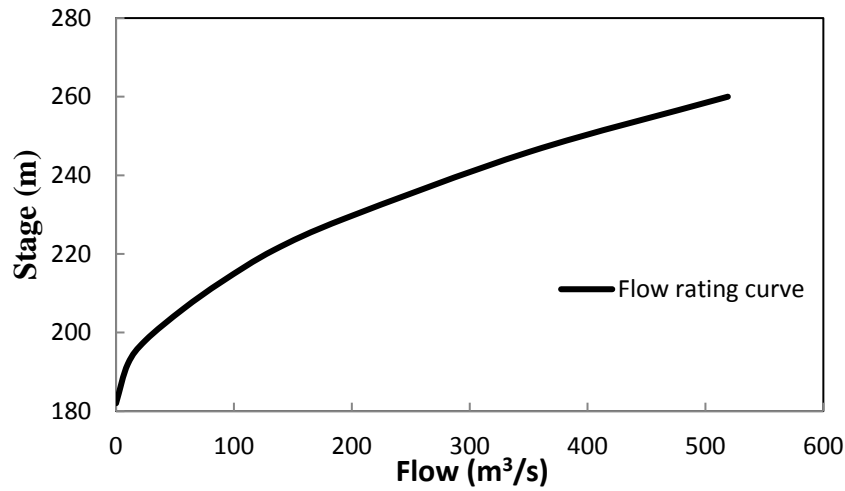


Figure 2: Schematic diagram of quasi-unsteady flow series with time step

The quasi-unsteady flow was selected due to its faster execution. Each steady flow profile was divided into three time steps such as computational increment, mixing time step and flow duration. Bathymetric changes and hydraulic parameters were kept constant throughout the mixing time step within a computational increment. The bathymetric changes due to the erosion and deposition of sediment changes the composition of bed mixing layers (active or inactive layers). The flow rating curve is the discharge-depth relationship of the dam and it was described in a simplified manner to yield the appropriate flow between the minimum and maximum water levels in the dam. The present study has considered flow series and rating curve as upstream and downstream flow boundary conditions. The direct runoff hydrograph (Beebo and Bilal, 2012) as shown in Fig. 3a was used as the upstream boundary condition at RS 100 and flow rating curve (Beebo and Bilal, 2012) as shown in Fig. 3b was used as the downstream boundary condition at RS 53.



(a)



(b)

Figure 3: (a) Upstream hydraulic boundary condition as flow time series at RS 100, (b) Hydraulic boundary condition at outlet (RS 53) - Flow rating curve

2.4.3. Sediment data

The sediment data includes sediment transport functions, particle fall velocity, bed gradation, sorting of bed sediment and boundary conditions which are described in this section. Several sediment transport functions are available in HEC-RAS for the computation of the sediment transport capacity. Besides this, the concentration of suspended sediment depends on particle fall velocity. The higher the fall velocity, the smaller the concentration and vice-versa. Fall velocity depends on Corey (1949) shape factor defined by $\phi = f / \sqrt{d}$ where d , b and f are longest, intermediate, and shortest axes of the particle treated as an ellipsoid, respectively. The relative mass density of particle was taken as 2.65 and the value of ϕ was taken as 0.6. Apart from this, the densities of sand, silt and clay were taken as 1489, 1041 and 480 kg/m³ respectively.

For each test reach in the model, the cross-sections are presented along with the invert elevation of the lowest point in each cross-section. This section also allows inputs for erodible cross-section limits which are assumed as 2 m interior for both the bank stations. One can control the limits of bed erosion of a cross-section by a maximum depth or a minimum elevation as well as making boundaries for the left or right bank (Brunner, et al., 2010). Maximum depth of sediment control volume was considered as 10 m. After setting the allowable scour area, a bed gradation curve can be inserted based on either percentage finer or grain-sizes fraction by weight. The bed gradation input in HEC-RAS was based on twenty predefined grain-sizes.

Bed sorting and armoring are possible in the bed layer. The sorting process available in HEC-RAS is the Exner-5 method which divides the bed layer into inactive layer and active layer or the sediment mixing layer. The active layer is further divided into cover layer and subsurface layer. The deposition and erosion of sediment occur in the cover layer; however, sediment transport computation is done in the subsurface layer for a given time step. The active layer thickness was assumed as the grain-size d_{90} which gives accurate results for the gravel bed.

2.4.4. Sediment Boundary Conditions

Sediment boundary condition controls the amount of sediment passing through a cross-section. The boundary condition is required for the first and last cross-sections and can be optionally applied to any additional cross-section. The sediment boundary condition options are equilibrium load, rating curve, point load, and distributed loads. These boundary conditions are useful in describing the very complex sediment loading in a system. Equilibrium load implies no aggradation or degradation, whereas the sediment rating curve indicates the amount of sediment load leaving from the system at a given time. At the end, HEC-RAS calculates the bed profile starting at the most downstream cross-section and marches in the upstream direction, making bed change calculations based upon transport function, sediment properties and other hydraulic parameters till it reaches the most upstream river station. For the Tenryu River model, an equilibrium load was selected for the upstream boundary condition (RS 100) and a sediment rating curve was selected for the downstream boundary condition (RS 53) as shown in Fig. 4.

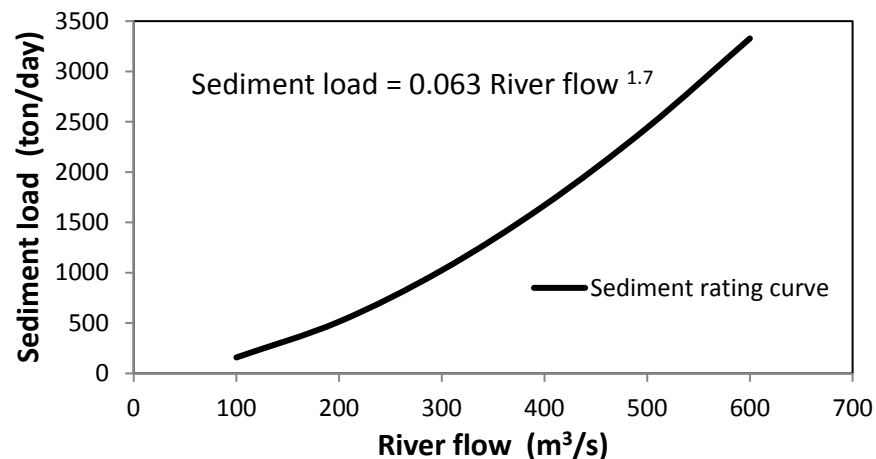


Figure 4: Sediment boundary condition at outlet – Sediment rating curve

3. Sakuma Dam

The Sakuma Dam is built for the hydropower generation on the Tenryu River. The length and height of the dam are 293.5 and 155.5 m respectively. The dam is located in Toyone city in the Kitashitara district on the border of Aichi Prefecture. The Sakuma Dam is a concrete gravity dam situated 70 km upstream of the river mouth. The Sakuma Dam was constructed between 1953 and 1956; however, its operations were started since 1957. The Hiraoka Dam is located upstream of 32 km from the Sakuma dam on the Tenryu River. The modeled region of the Tenryu River between the Hikora and Sakuma Dams is shown in Fig. 5.

According to Chaishi et al. (2002), the characteristics of the reservoir sedimentation of the Sakuma Dam are given as follows: a) catchment area 3800 Km^2 , b) reservoir capacity $3.26 \times 10^8 \text{ m}^3$, c) volume of accumulated sediment $1.12 \times 10^8 \text{ m}^3$ in which the active and dead storages are $0.45 \times 10^8 \text{ m}^3$ and $0.67 \times 10^8 \text{ m}^3$, respectively, d) average annual flow rate $79 - 171 \text{ m}^3/\text{s}$ and e) average specific sedimentation rate $685 \text{ m}^3/\text{km}^2/\text{year}$ after dam construction. Since 1957, the dam has been facing the severe sedimentation problems and resulting in the rapid reduction of storage capacity. It is observed that in a year, an average amount $2 \times 10^6 \text{ m}^3$ of sediment is retained. Palmieri et al. (2003) reported that the reservoir sedimentation caused a loss of 35% of the storage capacity of the Sakuma Dam reservoir by the year 2000. Due to the sediment retention, the life of the dam is reducing alarmingly as well as creating a severe erosion in the downstream of the dam. The water discharged from the Sakuma dam has lesser sediment concentration, therefore the flow is eroding the downstream river bed which has been degraded 1-1.5 m as reported by Sato and Liu (2008).

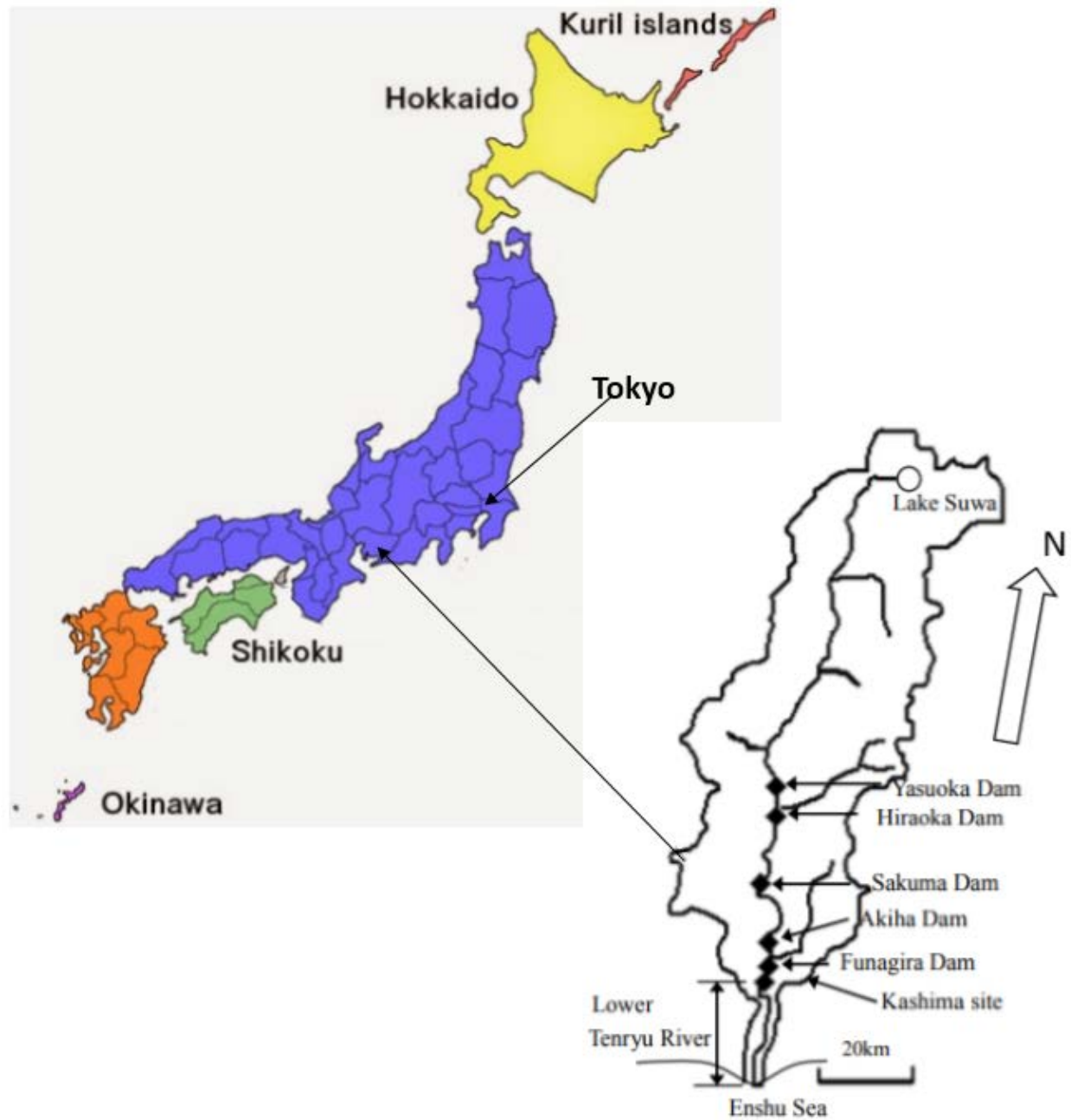


Figure 5: Tenryu River between the Hikora and Sakuma Dams.

4. Sedimentation modeling using HEC-RAS

In this section, the selection of modeling features required in HEC-RAS simulation is discussed. To specify the geometric data, the model section of the Tenryu River was divided into 48 river stations. A scaled plan view of the modeling region created by the HEC-RAS is shown in Fig. 6 and due to one-dimensional characteristic, only the sequence of the cross-sections can be seen. Satellite pictures of actual locations of cross-sections on the river are shown in Fig. 7. The most upstream cross-section, the river station (RS) 100 is located at the Hiraoka Dam and the most

downstream river station RS 53 is located at the Sakuma Dam. A not-to-scale schematic elevation diagram of the modeled region is shown in Fig. 8. The average distance between two river stations is about 680 m. After adding the coordinates of cross-sections, the data of the downstream test reach length of left over bank, main channel and right over bank are given as input. The Manning's roughness coefficient n was varied between 0.02 to 0.04 for LOB (Left Over Bank), main channel and ROB (Right Over Bank). The coefficients of contraction and extraction were considered as 0.1 and 0.3 respectively. It needs to be mentioned here that the trapezoidal geometrical shape was assumed for all cross-sections. The details of input geometric data to perform simulations are given in Table 1 (Beebo and Bilal 2012). The direct runoff hydrograph and flow rating curve of Beebo and Bilal (2012) were used as hydraulic boundary conditions at upstream RS 100 and downstream RS 53 respectively. For the fall velocity, the formula of van Rijn (1993) was used since it matches with the conditions of the Tenryu River (Brunner, 2002 a, b). Moreover, van Rijn (1993) used the shape factor as 0.7 which is the same as for natural sand (Jimenez and Madsen, 2003). The Exner-5 sorting method was chosen since it simulates the real sorting.

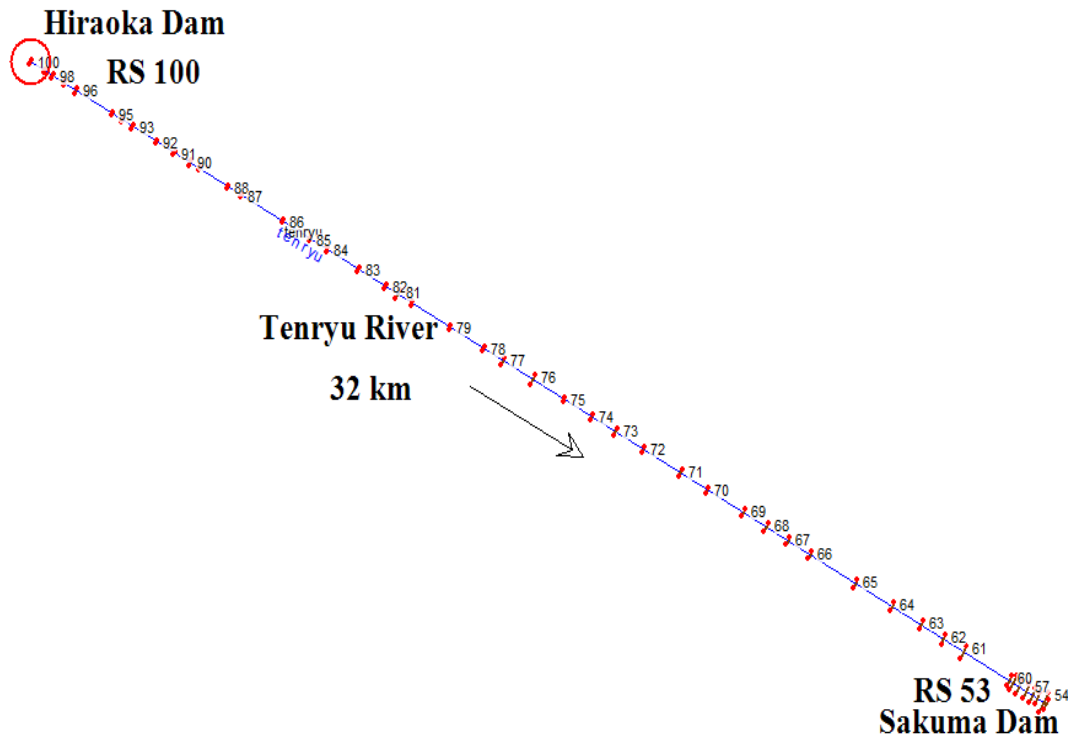


Figure 6: HEC-RAS generated scaled diagram of the modeled section of the Tenryu River with river stations

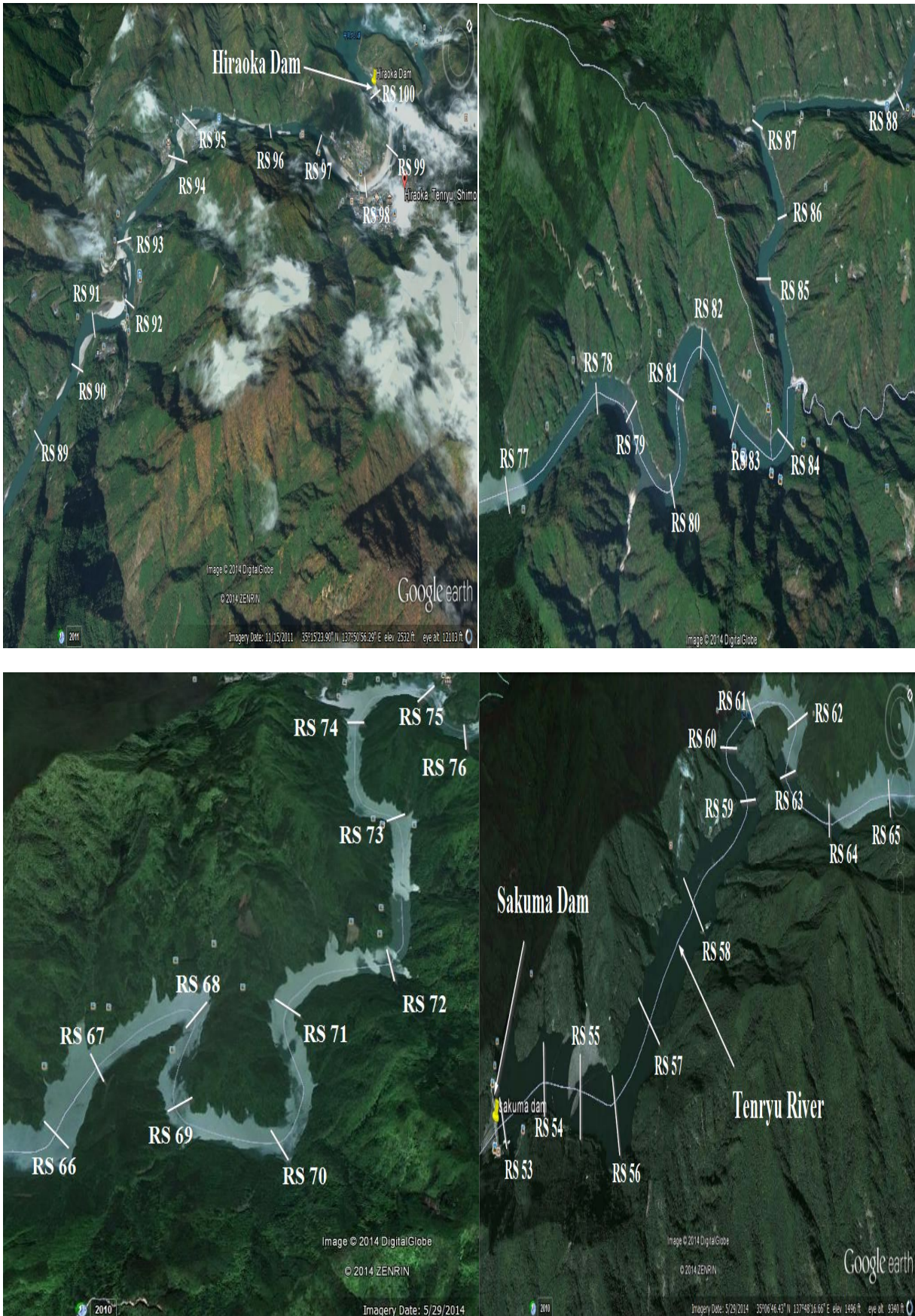


Figure 7: Cross section locations of the modeled reach of the Tenryu River (Google earth)

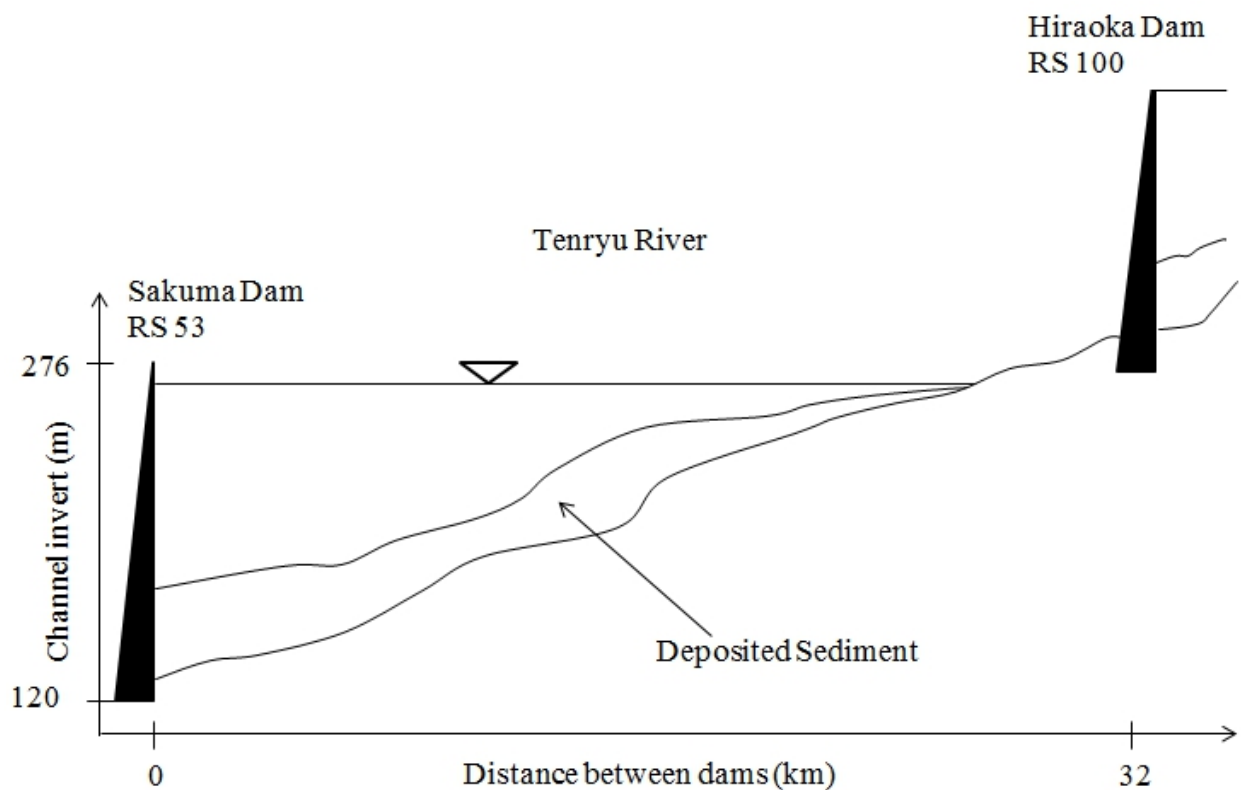


Figure 8: Schematic diagram of the model section and bed profile of the Tenryu River between the Hikora Dam and Sakuma Dam.

Table 1. Cross-sectional (stations and elevations) data of the river stations (RS) from 100 to 53

River station	Station (m)	Ele. (m)	Station (m)	Ele. (m)	Station (m)	Ele. (m)	Station (m)	Ele. (m)	Reach length LOB (m)	Reach length channel (m)	Reach length ROB (m)
100	5988	280.17	5994	260	6090	260	6098	280.17	450	450	450
99	5881	280.06	5888	259.3	5963	259.3	5971	280.06	314	252	395
98	5568	279.95	5575	259	5690	259	5698	279.95	353	378	404
97	5221	279.84	5228	258.5	5320	258.5	5328	279.84	422	379	310
96	4873	279.73	4879	258	4990	258	4999	279.73	1158	1162	1164
95	3946	279.62	3956	257	4026	257	4034	279.62	349	306	263
94	3776	279.51	3782	256.3	3847	256.3	3853	279.51	342	321	301
93	3996	279.4	4005	255.8	4106	255.8	4112	279.4	696	780	823
92	3938	279.29	3946	254.6	4030	254.6	4037	279.29	580	560	541
91	4399	279.18	4409	253	4480	253	4489	279.18	477	507	540
90	4199	279.07	4210	252.2	4330	252.2	4339	279.07	350	301	253
89	4350	278.96	4358	251.4	4417	251.4	4426	278.96	897	906	915

88	4506	278.85	4513	250.3	4558	250.3	4567	278.85	295	405	428
87	4266	278.74	4275	249	4334	249	4343	278.74	1360	1334	1309
86	3224	278.63	3230	247	3303	247	3311	278.63	922	890	859
85	3982	278.62	3988	244	4057	244	4062	278.62	426	522	535
84	4078	278.41	4085	242	4175	242	4183	278.41	981	1016	1052
83	4791	278.3	4798	238.3	4930	238.3	4937	278.3	826	852	878
82	3965	278.19	3973	237.6	4080	237.6	4090	278.19	465	393	330
81	3844	278.08	3852	237	4065	237	4073	278.08	464	441	428
80	4196	277.97	4204	236.4	4290	236.4	4301	277.97	1207	1220	1234
79	3087	277.86	3097	233	3210	233	3219	277.86	1111	1088	1065
78	2692	277.75	2699	228.3	2810	228.3	2821	277.75	556	607	659
77	2617	277.64	2629	220	2806	220	2817	277.64	960	948	936
76	1661	277.53	1669	214	1910	214	1921	277.53	1107	998	890
75	1430	277.42	1439	209	1560	209	1569	277.42	944	874	805
74	2139	277.31	2149	206	2290	206	2300	277.31	751	763	775
73	2882	277.2	2890	201	3048	201	3056	277.2	816	880	944
72	3446	277.09	3457	193	3600	193	3612	277.09	1170	1185	1201
71	2987	276.98	2994	188.5	3200	188.5	3209	276.98	901	872	844
70	3672	276.87	3680	180	3800	180	3814	276.87	1029	1135	1243
69	2764	276.76	2772	178	2958	178	2968	276.76	773	738	703
68	2159	276.65	2169	173	2397	173	2407	276.65	819	682	547
67	1880	276.54	1889	167	2075	167	2085	276.54	680	707	734
66	2117	276.43	2129	163	2334	163	2344	276.43	1306	1443	1580
65	1285	276.32	1287	158	1531	158	1533	276.32	1186	1174	1163
64	396	276.21	408	152	625	152	633	276.21	1094	928	764
63	100	276.1	110	150	334	150	342	276.1	721	710	700
62	692	275.99	699	146	944	146	952	275.99	562	638	719
61	596	275.88	607	141	930	141	939	275.88	1458	1447	1437
60	951	275.77	959	139	1207	139	1217	275.77	107	125	185
59	852	275.66	861	136	1240	136	1250	275.66	120	190	263
58	742	275.55	750	133.3	1117	133.3	1127	275.55	223	232	241
57	554	275.44	561	130.6	924	130.6	932	275.44	237	195	155
56	362	275.33	373	128	719	128	728	275.33	243	164	86
55	319	275.22	328	125.3	621	125.3	632	275.22	231	200	224
54	168	275.11	177	122.6	690	122.6	699	275.11	159	90	149
53	267	275	276	120	540	120	550	275	0	0	0

The bed gradation data of the Tenryu River in the year 1957 is not known; however Morris and Fan (1998) presented the bed gradation curves for the river bed in the year 1982. It is assumed initially that the bed gradation in the year 1957 is the same as in the year 1982. In the present study, four samples (O1, O2, O3 and O4) of bed gradation (Fig. 9) given by Morris and Fan

(1998) were considered as compared to Beebo and Bilal (2012) who considered only two bed gradation samples (O3, O4). The bed gradation samples are taken as 1) O4 in RS 100-RS 95, 2) O3 in RS 94-RS 85, 3) O2 in RS 84-RS 77 and 4) O1 in RS 76-RS 53 since Morris and Fan (1998) reported that the sediment size of the river bed decreases with increasing streamwise distance while specifying sediment data. HEC-RAS requires the width and vertical thickness (erodible limits) of control volume, which are not available in Beebo and Bilal (2012). In this study, the width was chosen as 2 m interior for the left and right bank stations, whereas the vertical thickness in terms of either maximum depth or minimum elevation was considered as 10 m. The vertical thicknesses of control volumes at each cross-section are given in Table 2. An equilibrium load was selected as the upstream sediment boundary condition at RS 100 and a sediment rating curve provided by Beebo and Bilal (2012) was taken as the downstream sediment boundary condition at RS 53.

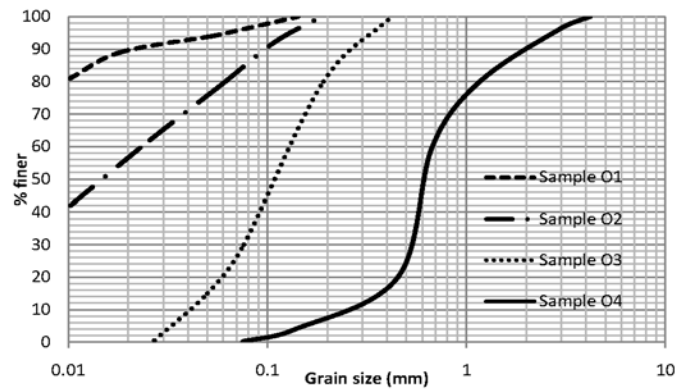


Figure 9: Four bed gradation curves of the Tenryu River collected in the 1982 by Morris and Fan (1998)

Table 2. Width and vertical thickness of control volume and bed gradation samples at different river Stations

RS ^a	CI ^b (m)	MD ^c (m)	ME ^d (m)	MCLL ^e	MCLR ^f	BGC ^g
100	260		260	6010	6116	O4
99	259.3		259.3	5903	5989	O4
98	259		259	5570	5696	O4
97	258.5		258.5	5223	5325	O4
96	258		258	4875	4997	O4
95	257		257	3948	4032	O4
94	256.3		256.3	3778	3851	O3
93	255.8		255.8	3998	4110	O3

92	254.6		254.6	3940	4035	O3
91	253		253	4401	4487	O3
90	252.2		252.2	4201	4337	O3
89	251.4		251.4	4352	4424	O3
88	250.3		250.3	4508	4565	O3
87	249		249	4268	4341	O3
86	247		247	3226	3309	O3
85	244		244	3984	4060	O3
84	242		242	4080	4181	O2
83	238.3		238.3	4793	4935	O2
82	237.6		237.6	3967	4088	O2
81	237		237	3846	4071	O2
80	236.4		236.4	4198	4299	O2
79	233		233	3089	3217	O2
78	228.3		228.3	2694	2819	O2
77	220		220	2619	2815	O2
76	214		214	1663	1919	O1
75	209		209	1432	1567	O1
74	206		206	2141	2298	O1
73	201		201	2884	3054	O1
72	193	10		3448	3610	O1
71	188.5		188.5	2989	3207	O1
70	180		180	3674	3812	O1
69	178	10		2766	2966	O1
68	173	10		2161	2405	O1
67	167		167	1882	2083	O1
66	163		163	2119	2342	O1
65	158	10		1287	1531	O1
64	152	10		398	631	O1
63	150		150	102	340	O1
62	146		146	694	950	O1
61	141		141	598	937	O1
60	139	10		953	1215	O1
59	136	10		854	1248	O1
58	133.3	10		744	1125	O1
57	130.6	10		556	930	O1
56	128		128	364	726	O1
55	125.3		125.3	321	630	O1
54	122.6		122.6	170	697	O1
53	120		120	269	548	O1

^aRiver station, ^bChannel invert, ^cMaximum Depth, ^dMinimum elevation, ^eMobile cross-sectional limit left,

^fMobile cross-sectional limit right and ^gBed gradation curve

5. Results and Discussion

The study of a thorough sensitivity analysis is difficult due to the availability of limited data regarding bed gradation curves of the Tenryu River. Bed gradation curves are available at only four river stations. Adjusting certain parameters on the Tenryu River model did provide some general information on sensitivity. In this analysis fall velocity method is chosen as Van Rijn based on shape factor of the particles present in the Tenryu River model. Rubey (1933) method is also used in the present research to model fall velocity. Exner-5 is chosen as sorting method. Bed gradation samples O1, O2, O3 and O4 at the river cross-sections are kept same throughout the simulations. After inputting the data in the HEC-RAS as discussed in Section 4, the effects of computational increment, sediment transport function, roughness coefficient, temperature of water, fall velocity and maximum depth of control volume are studied for their sensitivity on the bathymetric changes.

5.1. *Computational increment*

The numerical simulations of reservoir sedimentation are made with varying computational increment. In the simulations, sediment transport function, fall velocity and sorting method are kept constant. The computational increment is varied from 10 days to 6 hours and it is found that the simulation results are sensitive to the varying computational increment, therefore an optimum computational time step needs to be determined for a particular sediment transport function. The Engelund and Hasen (1967) transport function is selected because it is giving better results as compared to other sediment transport functions. Engelund and Hasen (1967) transport function is discussed in the next subsection. The computational increments are used as 10 days, 5 days, 24 hours, 18 hours, 15 hours, 12 hours, 9 hours and 6 hours. The comparisons between the computed results and available sediment spatial data in years 1975, 1998 and 2004 are shown in Fig. 10 and the same results are observed for the computational increments less than or equal to 24 hours. Therefore, the computational increment is selected as 24 hours in the present simulations.

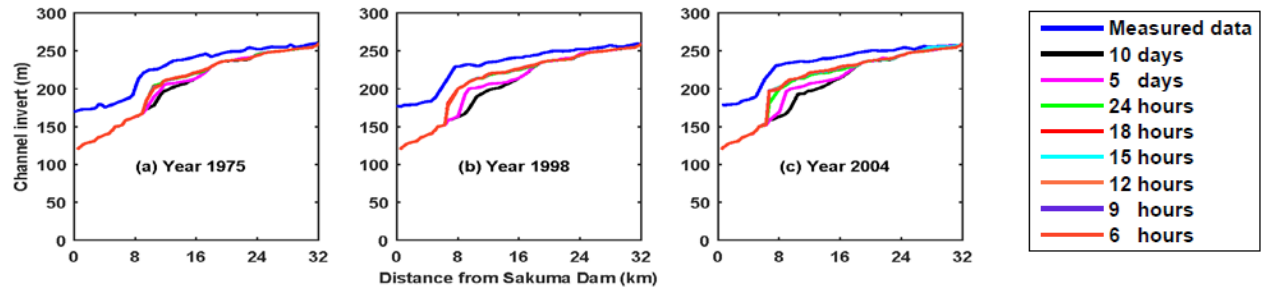


Figure 10: Comparison between observed and computed spatial plots for different computation increments in years a) 1975, b) 1998 and c) 2004.

5.2. Sediment transport function

The sediment transport functions used in the numerical simulations of the Tenryu River are 1) Meyer-Peter and Muller (1948), 2) Laursen (1958), 3) Engelund and Hansen (1967), 4) Toffaleti (1968), 5) Ackers and White (1973), 6) Yang (1973), 7) Wilcock and Crowe (2003) and 8) Wong and Parker (2006). The comparisons between the computed results and the measured data in years 1975, 1998 and 2004 are shown in Fig. 11. It is observed that the sediment transport function of Engelund and Hansen (1967), which is applicable for sandy river beds with sediment median size between 0.19 and 0.93 mm, is more accurate as compared to the other sediment transport functions. In contrary, Beebo and Bilal (2012) ranked the sediment transport functions of Toffaleti (1968) and Engelund and Hansen (1967) as first and second, respectively, for accurately predicting sediment transport in the Tenryu River between the Hikora and Sakuma Dams. In the present study, the sediment transport function of Wilcock and Crowe (2003) provides the next best result in comparison to Engelund and Hansen (1967). The Wilcock and Crowe (2003) method found to be sensitive to sand content in the bed on basis that decrease in sand content decreases the sediment transport.

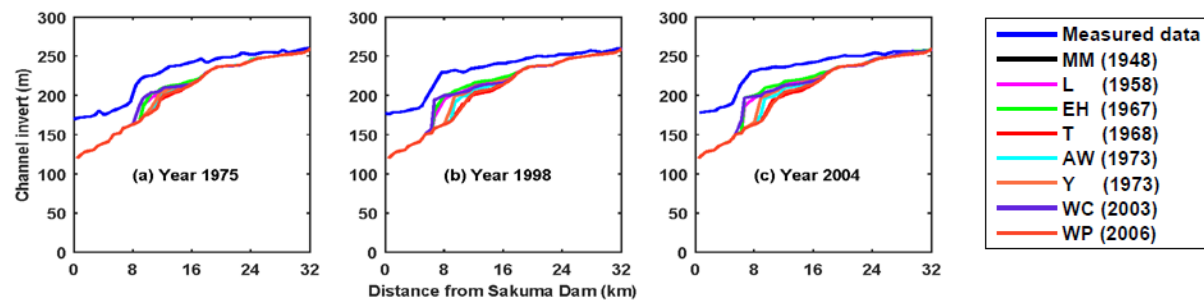


Figure 11: Comparison between observed and computed spatial plots for different sediment transport functions in years a) 1975, b) 1998 and c) 2004. The notations in legend are described

as MM (1948) for Meyer-Peter and Muller (1948), L (1958) for Laursen (1958), EH (1967) for Engelund and Hansen (1967), T (1968) for Toffaleti (1968), AW (1973) for Ackers and White (1973), Y (1973) for Yang (1973), WC (2003) for Wilcock and Crowe (2003) and WP (2006) for Wong and Parker (2006).

5.3. Manning's roughness coefficient

In the modeled region of the Tenryu River, the Manning's roughness coefficient n varies between 0.03 and 0.04 (Beebo and Bilal, 2012). In this study n is varied from 0.018 to 0.04 to investigate the effect of roughness on the reservoir sedimentation. The comparisons between the simulated results and the measured data in years 1975, 1998 and 2004 are shown in Fig. 12. It is found that the decreasing value of n from 0.04 to 0.02 leads the simulated bed profile closer to observed data and its further decreased value ($n = 0.018$) results in increasing the deviation between computed and observed profiles. Too low values of n are causing high erosion and resulting high sediment transport rates due to higher flow velocities. It is clear from Fig. 12 that $n = 0.02$ gives the most accurate comparison. Very important observation found in the present study is the nonlinear relation between Manning's roughness coefficient and reservoir sedimentation.

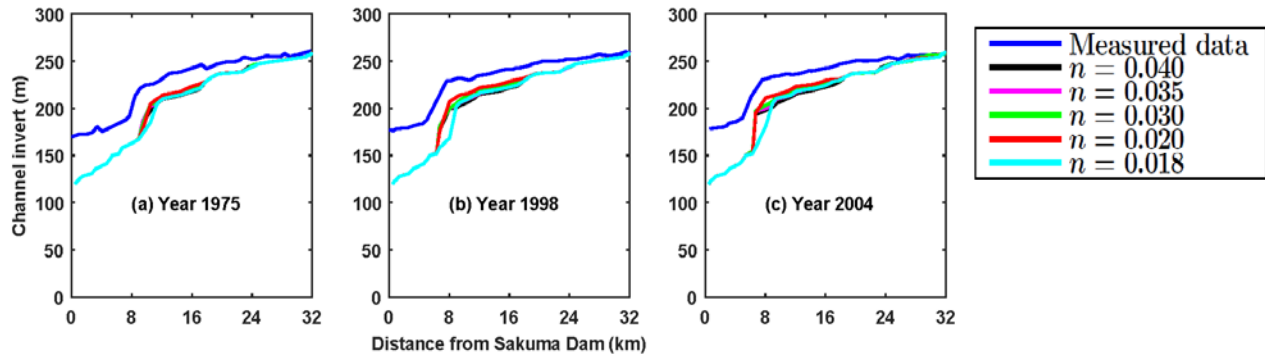


Figure 12: Comparison between observed and computed spatial plots for different Manning's roughness coefficients n in years a) 1975, b) 1998 and c) 2004.

5.4. Temperature of water

The viscosity of water is inversely proportional to its temperature. Hence, an increase or decrease in temperature has an effect on the bed shear stress as well as on the fall velocity of the sediment particle which depends on water viscosity. The bed shear stress increases with decreasing water temperature, therefore, lower temperature of flowing water produces higher erosion. Whereas sediment particle fall velocity increases with increase in temperature, i.e., sediment deposition increases with increase in temperature. Therefore, it may be concluded that higher reservoir

sedimentation occurs with higher water temperature in the reservoir. Beebo and Bilal (2012) considered the average monthly temperature, T in the region around Sakuma Dam as the temperature of flowing water in the Tenryu River. In addition, in the present study, the effect of temperature on the reservoir sedimentation in Sakuma Dam is studied by adding increments or decrements of 5°C ($T \pm 5$) to the local temperature. The comparisons between the simulated results and the measured bed profiles in 1975, 1998 and 2004 are shown in Fig. 13. It is observed that computed sediment spatial plot approaching the measured data of the Tenryu River with 5°C change in the local temperature. Further change in the temperature increased the deviation between computed and observed sediment bed spatial plots. The important finding in this study is that the influence of temperature on the sediment routing model is not significant. Beebo and Bilal (2012) found that the sediment transport function of Toffaleti (1968) which is a function of temperature (Brunner, 2010), gives better result. Therefore, according to Beebo and Bilal (2012), computed sediment spatial profiles have to be dependent on the temperature. In contrary, the present study demonstrated that reservoir sedimentation is independent of temperature.

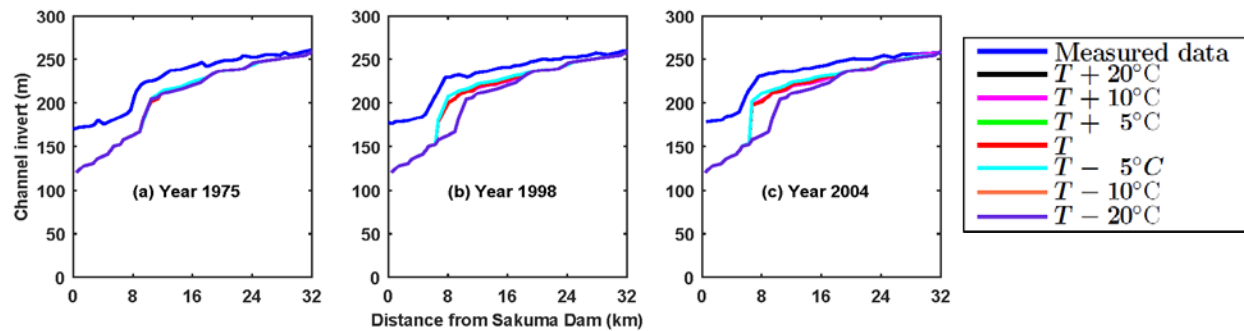


Figure 13: Comparison between observed and computed spatial plots for different temperatures T in years a) 1975, b) 1998 and c) 2004.

5.5. Fall velocity

The effect of fall velocity on the reservoir sedimentation is carried out for the specified sediment transport function of Engelund and Hansen (1967). The Manning's roughness coefficient and computational increment time are considered as 0.02 and 24 hours respectively. Exner-5 is used as sediment sorting method. Different theories of fall velocity considered in this study are 1) Rubey (1933), 2) Report-12 (1957), 3) Toffaleti (1968), 4) Dietrich (1982) and 5) van Rijn

(1993). The comparisons of simulated and the measured bed profiles in 1975, 1998 and 2004 are shown in Fig. 14.

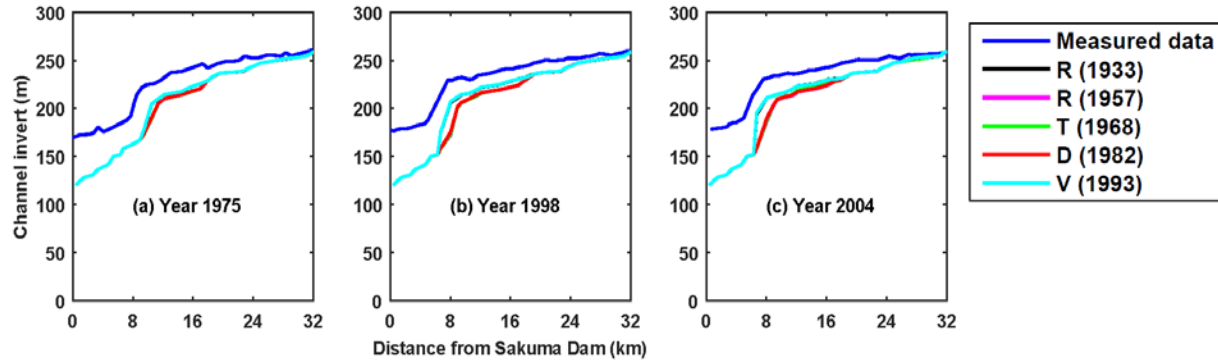


Figure 14: Comparison between observed and computed spatial plots for different fall velocities in years a) 1975, b) 1998 and c) 2004. The notations in legend are described as R (1933) for Rubey (1933), R (1957) for Report-12 (1957), T (1968) for Toffaleti (1968), D (1982) for Dietrich (1982) and V (1993) for van Rijn (1993).

It is clear from the figures that computed bed profiles with use of Van Rijn and Rubey fall velocity methods are better compared to other methods. Bed gradation in the modeled section of the Tenryu River falls in the range of natural sand which has a shape factor of 0.7 (Jimenez and Madsen, 2003). Van Rijn Fall velocity method uses a shape factor of 0.7 (Brunner, 2010) which could be the reason for its better performance. Results with Rubey model are as good as van Rijn model because both models designed for non-spherical silt, sand and gravel particles.

5.6. Sediment control volume dimensions

Previous consideration of maximum depth of 10 m at RS 57, 58, 59, 60, 64, 65, 68, 69 and 72 are changed to respective minimum channel elevations. Simulated profiles were compared with observed profiles by varying erodible widths from 1 m to 8 m at 2 m internal inwards to the bank stations and also compared with the profile of maximum erodible depth of 10 m. In this part of the study earlier obtained sensitive parameters of the model were not changed throughout the simulations. Fig. 15 shows that comparison between computed sediment spatial plots with erodible widths of 2 m and measured bed profiles is better than the other erodible limits.

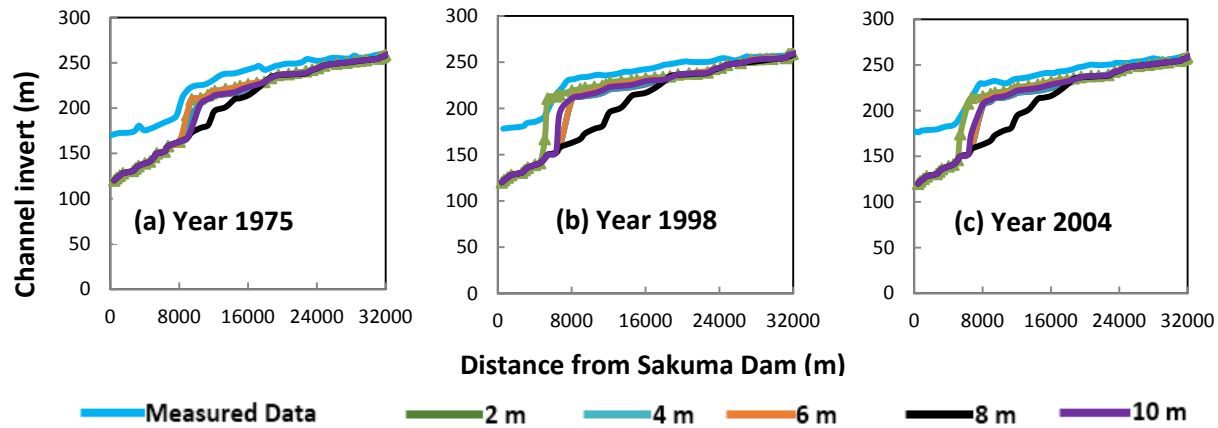


Figure 15: Comparison between observed and computed spatial plots for different erodible limits in years a) 1975, b) 1998 and c) 2004.

6. Conclusions

Numerical modeling of sediment transport using HEC-RAS is carried out for the Tenryu River between the Hiraoka and Sakuma Dams. The modeled length of the Tenryu River about 32 km is divided into 48 river stations and 47 reaches. The numerical simulations have been undertaken with varying sediment transport functions, computational increments, roughness coefficients, temperature of flow water and fall velocity models. The mathematical model is calibrated with the available monthly flows of 48 year data between 1957 and 2004. In the calibration study, the available bed gradation curves, channel geometry, Exner-5 sorting method, flow boundary conditions and sediment boundary conditions are kept constant. The computed bed profiles are compared with actual measured sediment bed spatial data for the years 1975, 1998 and 2004. The correct values of computational increment and Manning's roughness coefficient are identified as 24 hours and 0.02 respectively for the modeled section of the Tenryu River. In addition, the most suitable formulae of sediment transport function and fall velocity for the Tenryu River are found as Engelund and Hansen (1967) and van Rijn (1993) respectively. The Wilcock-Crowe (2003) formula also gave reasonable results next to Engelund-Hansen (1967) sediment transport function. The bathymetric changes computed using HEC-RAS are reasonable; however the occurrence of underestimated values might be due to unknown parameters such as locations of sluice gates, reservoir operating rules, presence of cohesive sediments, flow turbulence and the effect of the upper reservoir. A major finding in this study is that the temperature of water has no effect on the reservoir sedimentation. Although, Manning's

roughness coefficient has an effect on the sedimentation, no direct relation is found between the Manning's roughness coefficient and reservoir sedimentation. Van Rijn and Rubey fall velocity models are giving good results for sediment sizes available in the Tenryu River. Combination of Engelund-Hansen (1967) transport function, Manning's roughness coefficient of 0.02, computational increment of 24 hours, van Rijn fall velocity and erodible limits of 2 m gave the best comparison with the measured bed profile. Finally, it can be concluded that the present study is useful for the prediction of reservoir sedimentation in the Sakuma Dam.

Notations

A = Cross-sectional area

h = Depth of flow

Q = flowrate

Q_s = Sediment transport rate of size class i

V = Average channel velocity

S_f = Energy slope

d = Representative particle diameter

s_f = Particle shape factor

d_i = Geometric mean diameter of particles in size class i

T = Temperature of water

λ = Bed porosity

$\partial\eta$ = Change in bed level

x = Streamwise coordinate

t = Time step

Δx = Spatial step

η = Bed elevation

f = Dependent variable

α = Weighting factor

a = Length of particle along the longest axis perpendicular to the other two axes.

b = Length of particle along the intermediate axis perpendicular to the other two axes.

c = Length of particle along the short axis perpendicular to other two axes.

j, k = Grid coordinates

n = Manning's roughness coefficient

q_l = Volumetric rate of lateral inflow or outflow per unit length of the channel

References

Ackers, P., White, W.R., 1973. Sediment transport: new approach and analysis. *Journal of the Hydraulics Division* 99 (hy11).

Ahm, J., Yang, C., 2015. Determination of recovery factor for simulation of non-equilibrium sedimentation in reservoir. *International Journal of Sediment Research* 30 (1), 68-73.

Beebo, Q., Bilal, A. R., 2012. Simulating bathymetric changes in reservoirs due to sedimentation (tvvr-12/5018).

Brunner, G. W., 2002a. HEC-RAS river analysis system hydraulic reference manual, version 3.1, Hydrologic Engineering Center.

Brunner, G.W., 2002b. HEC-RAS river analysis system: User's manual. Hydrologic Engineering Center, US Army Corps of Engineers, Davis, California.

Brunner, Gary W., (2010), *HEC-RAS Hydraulic Reference Manual*. Davis CA, USA: US Army Corps of Engineer, Hydrological Engineering Center.

Caputo, M., Carcione, J.M., 2013. A memory model of sedimentation in water reservoirs. *Journal of Hydrology* 476, 426-432.

Chaishi, T., Kikuchi, T., Maeda, S., 2002. Accumulation of sediments in a reservoir and its countermeasures" a case study of Sakuma Dam". *Journal of the Japan Society of Engineering Geology* 43 (5), 316-319.

Chen, Ridong, Shao, Songdong, Liu, Xingnian, (2015), Water-sediment flow modeling for field case studies in Southwest China, *Natural Hazards*, 78(2), 1197-1224.

Ching-Hseinm W., Ching-Nuo, C., Chih-Heng, T., Chang-Tai, T., 2012. Estimating sediment deposition volume in a reservoir using the physiographic soil erosion-deposition model. *International Journal of Sediment Research* 27 (3), 362-377.

Corey, A. T., 1949. Influence of shape on the fall velocity of sand grains. Colorado State University.

Dietrich, W. E., 1982. Settling velocity of natural particles. *Water Resources Research* 18 (6), 1615-1626.

- Engelund, F., Hansen, E., 1967. A monograph on sediment transport in alluvial streams. Tech. rep., TEKNISKFORLAG Skelbregade 4 Copenhagen V, Denmark.
- Haq, I. U., Abbas, S.T., 2007. Sedimentation of Tarbela and Mangla reservoirs. In: Proceedings of the 70th Annual Session of the Pakistan Engineering Congress.
- Harb, G., 2013. Numerical modeling of sediment transport in alpine reservoirs. Dissertation of Doctor of Engineering Science, Graz University of Technology, Austria.
- Haun, S., Kjaerås, H., Løvfall, S., Olsen, N. R. B., 2013. Three-dimensional measurement and numerical modeling of suspended sediments in a hydropower reservoir. *Journal of Hydrology* 479, 180-188.
- Hosseinjanzadeh, H., Hosseini, K., Kaveh, K., Mousavi, S.F., 2015. New proposed method for prediction of reservoir sedimentation distribution. *International Journal of Sediment Research* 30 (3), 235-240.
- Huang, G., 2011. Dual behavior of suspended sediment concentration in a regulated river. *World Journal of Mechanics* 3 (1), 5775 (7 pages).
- Issa, I. E., Al-Ansari, N., Sherwany, G., Knutsson, S., 2016. Evaluation and modification of some empirical and semi-empirical approaches for prediction of area-storage capacity curves in reservoirs of dams. *International Journal of Sediment Research*.
- Ji, U., Jang, E. K., Kim, G., 2016. Numerical modeling of sedimentation control scenarios in the approach channel of the Nakdong river estuary barrage, South Korea. *International Journal of Sediment Research*.
- Jiménez, J. A., Madsen, O.S., 2003. A simple formula to estimate settling velocity of natural sediments. *Journal of waterway, port, coastal, and ocean engineering* 129 (2), 70-78.
- Lauer, J. W., Viparelli, E., Piegay, H., 2016. Morphodynamics and sediment tracers in 1-d (mast-1d): 1-d sediment transport that includes exchange with an off-channel sediment reservoir. *Advances in Water Resources*.
- Laursen, E. M., 1958. The total sediment load of streams. *Journal of the Hydraulics Division* 84 (1), 1-36.
- Meyer-Peter, E., Muller, R., 1948. Formulas for bed-load transport. *IAHR*.
- Miyahara, S., Uda, T., Furuike, K., Serizawa, M., San-nami, T., Ishikawa, T., 2010. Effect of sand bypassing at Sakuma dam in the Tenryu River as a measure against erosion of the Tenryu River delta coast. *Coastal Engineering Proceedings* 1 (32), 12 pages.
- Molinas, A., Yang, C. T., 1986. Computer program user's manual for GSTARS. US Bureau of Reclamation Engineering and Research Center, Denver, CO 80225.

Morris, Gregory L. and Fan, Jiahua. 1998. Reservoir Sedimentation Handbook, McGraw-Hill Book Co., New York.

Okano, M., Kikui, M., Ishida, H., Sumi, T., 2005. Study on reservoir sediment excavation management and sediment replenishment to downstream rivers. Journal of Japan Society of Dam Engineers 15 (3), 200-215.

Palmieri, A., Shah, F., Annandale, G. W., Dinar, A., 2003. Reservoir conservation volume in the rescon approach economic and engineering evaluation of alternative strategies for managing sedimentation in storage reservoirs.

Report-12, 1957. Some fundamentals of particle size analysis: A study of methods used in measurement and analysis of sediment loads in streams. Tech. rep., Inter-Agency Committee of Water Resources and St. Anthony Falls Hydraulic Laboratory, Minneapolis, Minnesota, USA.

Rubey, W. W., 1933. Settling velocity of gravel, sand, and silt particles. American Journal of Science (148), 325-338.

Sato, S., Liu, H., 2008. A comprehensive study on sediment movement in Tenryu River watershed and Enshu coast.

Toffaleti, F. B., 1968. A procedure for computation of the total river sand discharge and detailed distribution, bed to surface. Tech. rep., DTIC Document.

Tsai, C. W., Hsu, Y., Lai, K. C., Wu, N. K., 2014. Application of gamblers ruin model to sediment transport problems. Journal of Hydrology 510, 197-207.

Van Rijn, L. C., 1993. Principles of sediment transport in rivers, estuaries and coastal seas. Vol. 1006. Aqua publications Amsterdam.

Wilcock, P. R., Crowe, J. C., 2003. Surface-based transport model for mixed size sediment. Journal of Hydraulic Engineering 129 (2), 120-128.

Wong, M., Parker, G., 2006. Reanalysis and correction of bed-load relation of Meyer-Peter and Muller using their own database. Journal of Hydraulic Engineering 132 (11), 1159-1168.

Yang, C. T., 1973. Incipient motion and sediment transport. Journal of the Hydraulics Division 99 (10), 1679-1704.

Yang, C.T., 2006. Erosion and sedimentation manual. US Dep. of the Interior, Bureau of Reclamation, Denver, CO.

Yin, K, X., S, H., W, 2016. Modeling sediment concentration and transport induced by storm surge in Hengmen Eastern Access Channel (HEAC). Nat Hazards 82, 617-642.